*Proceedings of ITC18,2008*

# Conceptual Design of dispersion interferometer using ratio of modulation amplitudes

T. Akiyama, K. Kawahata, S. Okajima[a] and K. Nakayama[a]

*National Institute for Fusion Science, 322-6 Oroshi-cho, Toki 509-5292, Japan*

[a)] *Chubu University, 1200, Matsumoto-cho,Kasugai 487-8501, Japan*

Since a dispersion interferometer is free from mechanical vibrations, it does not need a vibration compensation system even if a wavelength of a probe beam is short (e.x. infrared and near infrared region). This paper describes a new signal processing of the dispersion interferometer using a ratio of modulation amplitudes with a photoelastic modulator. The proposed method is immune to changes in detected signal intensities and the signal processing system becomes simple. Designs of the optical system of the dispersion interferometer for proof of principle, especially specification of a nonlinear optical crystal, are also shown.

Keywords: interferometer, dispersion interferometer, non-linear crystal, photoelastic modulator, $CO_2$ laser

## 1. Introduction

High reliability and resolutions are required for electron density measurements in fusion devices in order to control plasmas and to understand the plasma physics.

A conventional heterodyne interferometer is widely used for the electron density measurement and has a high density resolution. It, however, suffers from fringe jump errors, which degrade reliability of the interferometer, in a high density range. These days the Large Helical Device (LHD) developed a high density operation regime whose central electron density is up to several times $10^{20}$ $m^{-3}$ [1], and the expected density range in ITER is about 1 $\times 10^{20}$ $m^{-3}$ [2]. Hence the problem of the fringe jump is becoming more significant. While a short-wavelength laser can reduce probabilities of the fringe jumps, phase errors caused by mechanical vibrations become significant. They should be suppressed with a vibration isolator or be compensated by adopting the two-color interferometry, which consists of two probe beams with different wavelengths (light sources). Even so, it is difficult to eliminate the vibration components completely because of slight differences in the optical path and wavefronts of probe beams and an optical system becomes complex and expensive.

One candidate of the solutions is a density measurement with a polarimeter based on the Faraday effect [3-5] or the Cotton-Mouton effect [6-8]. Although density resolutions of polarimeters are less than these of the interferometers, it does not suffer from fringe jump errors and immune to mechanical vibrations principally. The other candidate is a dispersion interferometer [9]. It is also insensitive to mechanical vibrations and hence does not need the vibration isolator and the two-color interferometry system even if the short-wavelength laser, for example a $CO_2$ laser and a YAG laser, is used.

This paper describes a new signal processing of the dispersion interferometer using a ratio of modulation amplitudes. The proposed method makes the signal processing simple and can remove measurement errors due to changes in the detected signal intensity. Section 2 briefly explains the principle of the dispersion interferometer and the new proposed signal processing. Section 3 shows a design of the proposed dispersion interferometer for the proof of the principle. Summaries are given in Sec. 4.

## 2. Principle of dispersion interferometer

### 2.1. Basic dispersion interferometer

Figure 1 shows the principle of the basic dispersion interferometer [9]. A probe beam whose angular frequency is $\omega$ passes through a type-I nonlinear crystal to generate the second harmonic whose polarization angle is perpendicular to that of the fundamental. And then, the fundamental and the second harmonic components propagate along almost the same optical path. Phase shifts due to changes in the optical path length $\Delta d$ by

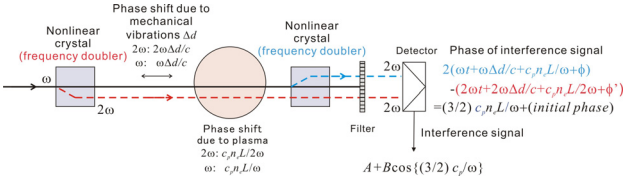


Fig.1 Basic dispersion interferometer

*author's e-mail: takiyama@lhd.nifs.ac.jp*

mechanical vibrations are $\omega\Delta d/c$ and $2\omega\Delta d/c$, respectively. The phase shifts due to a plasma are $c_p\bar{n}_eL/\omega$ and $c_p\bar{n}_eL/(2\omega)$, where $c_p = e^2/(2\varepsilon_0 m_e c)$, $\bar{n}_e$ is the line averaged electron density and $L$ is the optical path length in the plasma. After passing through the plasma the frequency of the fundamental wave is doubled again with the other nonlinear crystal. The remaining fundamental, which is not converted into the second harmonic, is cut by a following filter and the second harmonic components only go into a detector. Phases of these second harmonic components $\varphi_1$ and $\varphi_2$ (second harmonics which are generated by the first and the second nonlinear crystals are noted as 1 and 2, respectively) are given as follows:

$$\begin{aligned}\varphi_1 &= 2(\omega t + \omega\Delta d/c + c_p\bar{n}_eL/\omega + \phi_1)\\ \varphi_2 &= 2\omega t + 2\omega\Delta d/c + c_p\bar{n}_eL/(2\omega) + \phi_2\end{aligned} \quad (1)$$

where $\phi_1$ and $\phi_2$ are initial phases of second harmonics. The detected interference signal $I$ between these second harmonic components becomes

$$\begin{aligned}I &= A + B\cos(\varphi_1 - \varphi_2)\\ &= A + B\cos\left(\frac{3}{2}\frac{c_p\bar{n}_eL}{\omega} + \phi\right).\\ A &= I_1 + I_2,\ B = 2\sqrt{I_1I_2}\\ I_1, I_2 &: \text{intensities of second components}\\ \phi &= \phi_1 - \phi_2 : \text{initial phase}\end{aligned} \quad (2)$$

As shown in Eq. (2), the phase shift due to mechanical vibrations is canceled out automatically. Hence, the phase of the interference signal is determined by only the dispersion of the plasma and is free from mechanical vibrations even with a short wavelength laser.

## 2.2. Dispersion interferometer with a phase modulation

Since Eq. (2) is the almost the same as the interference signal of a homodyne interferometer, the basic dispersion interferometer has the same disadvantage as the homodyne one: (i) restriction of the phase where Eq. (2) is a monotonic function (ii) necessity of calibration experiments of the detected intensity $A$ and $B$ and their variations during discharges lead to phase errors. The phase modulation method [10] with an electro-optical modulator (EOM) can reduce the influence of the intensity variations. The EOM, which is operated with a drive signal of $\pi\sin\Omega t$, is inserted between the first nonlinear crystal and the plasma. It gives a phase modulation of $\pi\sin\Omega t$ only for the second harmonic components. As a result, the following modulated interference signal $I_{pm}$ is detected.

$$I_{pm} = A + B\cos\left(\pi\sin\Omega t + \frac{3}{2}\frac{c_p\bar{n}_eL}{\omega} + \phi\right) \quad (3)$$

$I_{pm}$ is directly digitized with a higher sampling frequency than $\Omega$. Due to the phase modulation the amplitude of $I_{pm}$ changes between maximum ($A$+$B$) and the minimum ($A$-$B$). $A$ and $B$ are assumed constants during one modulation period and the DC component $A$ and the amplitude $B$ are evaluated from the digitized signal. And then, $A$ is subtracted from the digitized signal and the amplitude of $I_{pm}$ is normalized by $B$. The drive signal of the EOC is also digitized coincidently and the times $t_0$ when $\sin\Omega t_0 = 0$ are determined. At the $t_0$, normalized signal $I_{pm}^{norm}$ becomes

$$I_{pm}^{norm} = \cos\left(0 + \frac{3}{2}\frac{c_p\bar{n}_eL}{\omega} + \phi\right). \quad (4)$$

The line averaged electron density can be calculated from the arcosine of Eq. (4).

## 2.3. Dispersion interferometer using a ratio of modulation amplitudes

Now we are designing a dispersion interferometer with a use of a photoelastic modulator (PEM) instead of

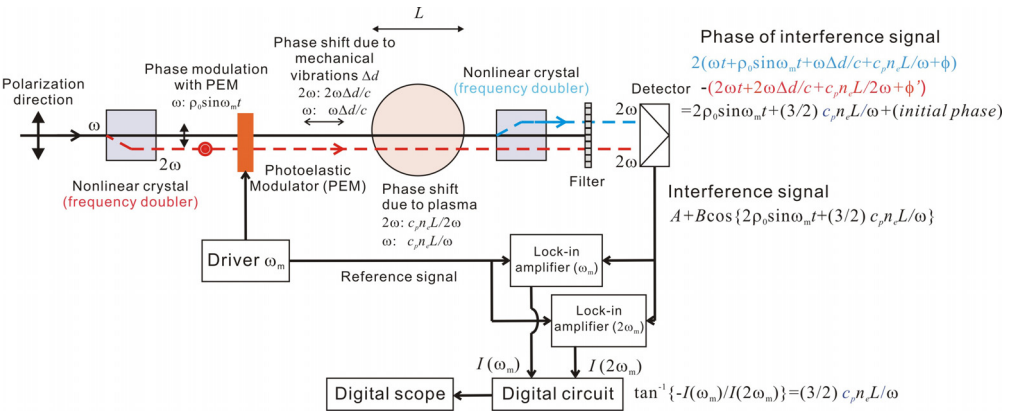


Fig.2 Dispersion interferometer with a photoelastic modulator (PEM) and a signal processing using ration of modulation amplitudes

the EOM, whose modulation frequency is stable. Figure 2 shows the schematic view. The modulator axis of the PEM is arranged parallel to the polarization direction of the fundamental in order to give phase modulations only to the fundamental. In this configuration, the following interference signal $I(t)$ is obtained.

$$\begin{aligned} I(t) &= A + B\cos\left(2\rho_0 \sin\omega_m t + \frac{3}{2}\frac{c_p \bar{n}_e L}{\omega} + \phi\right) \\ &= A + B\left\{\cos(2\rho_0 \sin\omega_m t)\cos\left(\frac{3}{2}\frac{c_p \bar{n}_e L}{\omega} + \phi\right)\right\} \\ &\quad - B\left\{\sin(2\rho_0 \sin\omega_m t)\sin\left(\frac{3}{2}\frac{c_p \bar{n}_e L}{\omega} + \phi\right)\right\} \end{aligned} \quad (5)$$

where $\rho_0$ is the maximum retardation of the PEM, which is determined by the applied voltage to the PEM, $\omega_m$ is the modulation frequency of the PEM. Here, $\cos(2\rho_0 \sin\omega_m t)$ and $\sin(2\rho_0 \sin\omega_m t)$ can be expanded with the Bessel function of order of n $J_n$.

$$\begin{aligned} \cos(2\rho_0 \sin\omega_m t) &= J_0(2\rho_0) + 2\sum_{n=1}^{\infty} J_{2n}(2\rho_0)\cos(2n\omega_m t) \\ \sin(2\rho_0 \sin\omega_m t) &= 2\sum_{n=1}^{\infty} J_{2n-1}(2\rho_0)\sin\{(2n-1)\omega_m t\} \end{aligned} \quad (6)$$

In this way, the detected interference signal $I(t)$ can be expanded with harmonic components of $\omega_m$. The following amplitudes of fundamental and the second harmonic components $I_{\omega_m}$ and $I_{2\omega_m}$ of the modulation frequency $\omega_m$ can be measured with lock-in amplifiers.

$$\begin{aligned} I_{\omega_m} &= -2BJ_1(2\rho_0)\sin\left(\frac{3}{2}\frac{c_p \bar{n}_e L}{\omega}\right) \\ I_{2\omega_m} &= 2BJ_2(2\rho_0)\cos\left(\frac{3}{2}\frac{c_p \bar{n}_e L}{\omega}\right) \end{aligned} \quad (7)$$

From the ratio of these amplitudes, the line averaged electron density $\bar{n}_e$ is obtained.

$$\begin{aligned} \frac{I_{\omega_m}}{I_{2\omega_m}} &= \tan\left(\frac{3}{2}\frac{c_p \bar{n}_e L}{\omega}\right) \\ \therefore \bar{n}_e &= \frac{2}{3}\frac{\omega}{c_p L}\tan^{-1}\left\{\frac{I_{\omega_m}}{I_{2\omega_m}}\right\} \end{aligned} \quad (8)$$

Here, $\rho_0$ is set at 1.3 radian by applying the adequate voltage to the photoelastic material for $J_1(2\rho_0) = J_2(2\rho_0)$. This new method of the phase extraction is completely free from variations of detected intensities $A$ and $B$. In addition, it is simpler than that in Ref [10] and suits to real time measurements.

Table 1 Optical parameters of $AgGaSe_2$ for 10.6 μm

| | |
|---|---|
| Transparency (μm) | 0.8-18 |
| Refractive index $n_o$ (10.6 μm) | 2.5912 |
| Refractive index $n_e$ (10.6 μm) | 2.5579 |
| Refractive index $n_o$ (5.3 μm) | 2.1634 |
| Refractive index $n_e$ (5.3 μm) | 2.5808 |
| Phase-matching angle (deg.) | 55.4 |
| $d_{eff}$ (definition: $P=dE^2$) | $2.47\times10^{-22}$ |
| Surface damage threshold $P_{sd}$ ($kW/cm^2$, CW) | 33-45 |
| Thermal-lensing threshold $P_l$ ($kW/cm^2$) | 2 |
| Thermal conductivity (W/cm/K) | 0.011 |
| Absorption coefficient ($cm^{-1}$) | 0.09 |

## 3. Conceptual design of dispersion interferometer using a ratio of modulation amplitude

For the proof of the principle, we are designing a dispersion interferometer with a $CO_2$ laser whose wavelength is 10.6 μm. The $CO_2$ laser to be used is GN-802-GES with an output power (MPB Technology Inc.) of 7.5W or LC-25 (DEOS) with 25 W. Either one of them will be selected according to a signal-to-noise ratio (SNR). One of important components for good SNR is the nonlinear crystal for second-harmonic generation (SHG) because the power of the second harmonics strongly depends on the specifications of the nonlinear crystal.

### 3.1. Design of a nonlinear crystal for SHG

Silver gallium selenide ($AgGaSe_2$) is commonly used for SHG of 10.6 μm laser light. Table 1[11, 12] summarizes properties of $AgGaSe_2$. The conversion efficiency $\eta = P_{2\omega}/P_{\omega}$, where $P_{2\omega}$ and $P_{\omega}$ are the powers of the second harmonic and the fandamental, is given by [13]

$$\eta = 2\left(\frac{\mu}{\varepsilon_0}\right)^{3/2}\frac{\omega^2 {d_{\text{eff}}}^2 l^2}{n^3}\left(\frac{P_\omega}{\pi\omega_0^2}\right)\left\{\frac{\sin(\Delta k l/2)}{\Delta k l/2}\right\}^2 \quad (9)$$
$$\Delta k \equiv k_{2\omega} - 2k_{\omega}$$

where $\omega$ is the laser frequency, $d_{\text{eff}}$ is the effective nonlinearity, $l$ is the length of the crystal, $n$ is the refractive index of the fundamental, $\omega_0$ is the beam waist, $k_{2\omega}$ and $k_{\omega}$ are wavenumbers of the second harmonics and the fundamental, respectively. The last term, which includes $\Delta k$, stands for the phase matching condition. As is mentioned in Sec. 3.2, that is determined by the angle between the beam path and the optic axis of the crystal. Here, the phase matching condition is assumed to be satisfied and the term is given to be unity. It is noted that Eq. (9) presumes a plane wave for an incident light. This is approximately valid when the length of the crystal is less than the confocal focusing length $z_0 = \pi\omega_0^2 n/\lambda$ of the Gaussian beam.

Generally, $\eta$ of the second harmonic of a continuous-wave laser light is small, an order of 0.1%. Hence, it is favorable for good SNR to increase the power of the second harmonic as much as possible. Eq. (9)

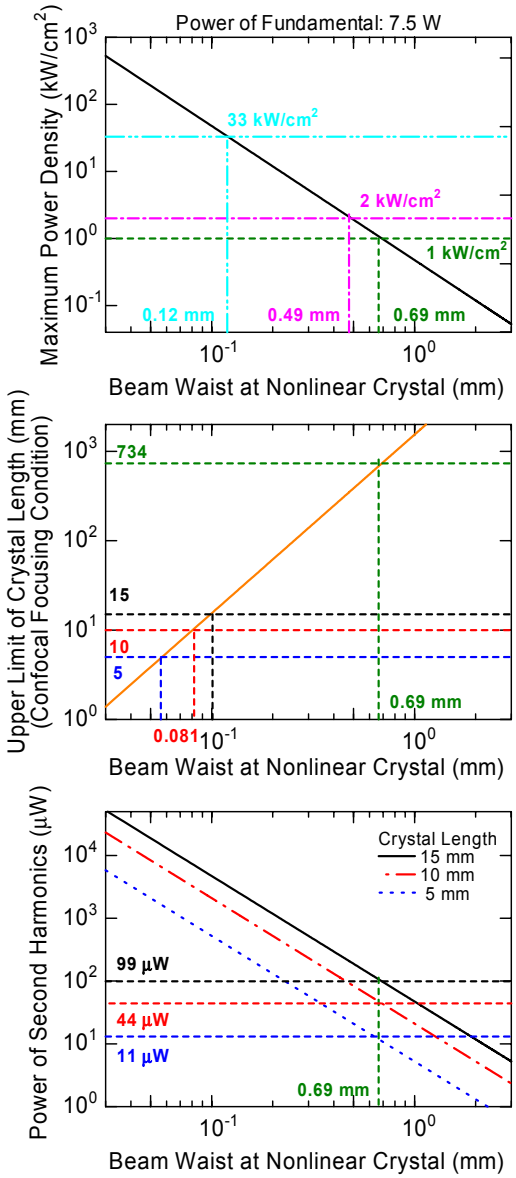


Fig.3 Dependence of (a) maximum power density, (b) upper limit of crystal length and (c) power of second harmonic component on a beam waist at a nonlinear crystal in the case of an incident beam with a power of 7.5 W. The nonlinear crystal is $AgGaSe_2$.

indicates that $\eta$ increases with the power density of the incident beam. However, there are some following limitations in the power density and the crystal length.

The maximum power density $P_0 = 2P_{total} / (\pi\omega_0^2)$ of the focused Gaussian beam into the nonlinear crystal should be smaller than a surface damage threshold $P_{sd}$ of 33 kW/cm$^2$ for a cw laser. Here, $P_{total}$ is the total incident power and $\omega_0$ is the beam waist (1/e$^2$ power radius). In the case of $AgGaSe_2$, the thermal-lensing effect, which decreases the SHG efficiency, should be considered. This is due to the small thermal conductivity, which is comparable to glass, for example. A threshold $P_l$ for the thermal-lensing effect of 2 kW/cm$^2$ reported in Ref. 11 and is smaller than $P_{sd}$, allowable beam waist is determined by $P_l$. In this design, the maximum power density is set at the half of $P_l$, 1 kW/cm$^2$, for safety. The resultant beam waist focused in the center of the crystal is 0.69 mm as shown in Fig. 1(a) for a total incident power of 7.5 W.

The commercially available length of the $AgGaSe_2$ crystal is up to 20 mm at present. The upper limit of the crystal length which is determined by the confocal focusing length is much larger than available length for a beam waist of 0.69 mm as shown in Fig.1(b).

Figure 1(c) shows the power of the generated second harmonic calculated with Eq. (9). In the case of 15 mm-long crystal, 99 μW is generated from an incident beam with a power of 7.5 W and with a beam waist of 0.69 mm. The transmissivity at the second harmonic of zinc sellenide ZnSe with anti-reflection coating at the fundamental, which is used for the PEM and two vacuum windows (not shown in Fig.2), is about 0.65. That of IR filter made of sapphire which eliminates the fundamental (see Fig.2) is about 0.7. Hence the total transmissivity of the second harmonics which is generated in the first nonlinear crystal is $0.65^3*0.7=0.19$. When the thermoelectrical cooled IR photovoltaic detector PVI-3TE-5 (Vigo system, Responsivity: 2 (A/W)) with the preamplifier STCC-04 (Vigo system, Transimpedance: $10^5$ (V/A)) are used, the output voltages $I_1$ and $I_2$ becomes as follows.

$I_1 = (99*10^{-6})*0.19*2*10^5 = 3.8$ V

$I_2 = (99*10^{-6})*0.7*2*10^5 = 14$ V

Considering the efficiency of interference and reflectivity of mirrors and so on, the detected power will be slightly smaller. Nevertheless, these generated powers of the second harmonics are enough to be detected.

### 3.2. Phase matching condition

The second harmonic is continuously generated along the optical path in the nonlinear crystal. If phases of the second harmonic which is generated at the entrance region and the central region in the crystal, they interfere each other and the total power of the second harmonic decreases. In order to suppress that, the phase of the second harmonic should be matched (phase matching condition). For that purpose, the fundamental is injected into the crystal in the certain angle $\theta_m$ against the optic axis of the crystal to satisfy $n_e^{(2\omega)} = n_o^{(\omega)}$ based on the birefringence. In the case of the type-I nonlinear crystal, which is used in this dispersion interferometer, the fundamental and the second harmonic are ordinary and extraordinary wave, respectively. $\theta_m$ is given by following expression [13].

$$\sin^2\theta_m = \frac{\left\{n_o^{(\omega)}\right\}^{-2} - \left\{n_o^{(2\omega)}\right\}^{-2}}{\left\{n_e^{(2\omega)}\right\}^{-2} - \left\{n_o^{(2\omega)}\right\}^{-2}} \quad (10)$$

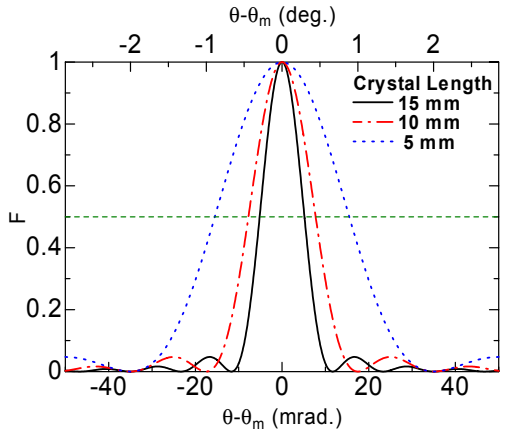


Fig.4 Phase matching condition for $AgGaSe_2$

Assigning refractive indexes, $\theta_m$ of $AgGaSe_2$ becomes 55.4 deg. $\Delta k$ is also given by

$$\Delta kl/2 = \frac{\omega l}{c}\left\{n_e^{(2\omega)}(\theta_m) - n_o^{(\omega)}\right\} \approx -\frac{\omega l}{c}\sin(2\theta_m)\frac{\left\{n_e^{(2\omega)}\right\}^{-2} - \left\{n_o^{(2\omega)}\right\}^{-2}}{2\left\{n_o^{(\omega)}\right\}^{-3}}(\theta - \theta_m) \quad (11)$$

and $F = \left\{\sin(\Delta kl/2)/(\Delta kl/2)\right\}^2$ is plotted in Fig. 4. The half width of $F$ for the 15-mm long crystal is only 0.3 deg. Since a beam deviation angle of the $CO_2$ laser beam caused by a density gradient is an order of 0.01 deg. in the case of a LHD plasma with a density profile of $1\times10^{20}$ $(1-\rho^8)$ $m^{-3}$, for example. However, it should be pay attention to the reduction of the power of the second harmonic in the high density range where the beam deviation angle becomes large.

3.3. Temperature raise of the nonlinear crystal

The temperature of the nonlinear crystal raises due to absorption of the laser power. The absorbed power $P_{abs}$ is given by

$$P_{abs} = P_{total}\left[1-\exp(-\alpha l)\right] \quad (12)$$

where $\alpha$ is an absorption coefficient. 0.09 $cm^{-1}$ is reported for $AgGaSe_2$, then $P_{abs}$ becomes 0.95 W. The heat balance between the crystal and surrounding air is written by

$$T = T_0 + P_{abs}/(hS) \quad (13)$$

where $h$ is the heat transfer coefficient, $S$ is the surface area of the crystal, $T$ is the crystal temperature, $T_0$ is the air temperature (here, 27°C). Assuming the heat transfer coefficient is 10 $Wm^{-2}K^{-1}$ pessimistically, the crystal temperature raises up to 371°C for the 5×5×15 mm-size crystal ($S$=2.25 $cm^2$ excluding the bottom plane 5×15 $mm^2$). In case that the surface area is increased up to 50 $cm^2$ by attaching a heat sink, the crystal temperature is only 47°C. Although the temperature is uniform inside the crystal in this rough estimation, the small thermal conductivity of $AgGaSe_2$ makes heat gradient between the central region and the surface. Hence it is necessary to have enough temperature margins for designing of the heat sink and cooling.

## 4. Summary

A dispersion interferometer is one of candidates of reliable electron density measurement. We propose the dispersion interferometer using a ratio of modulation amplitudes with a PEM. This method removes measurement errors from changes in the detected signal intensity and makes the signal processing simple and easy to use for real time feedback control. $AgGaSe_2$ is selected for SHG of a $CO_2$ laser dispersion interferometer for proof of the principle and the power of the generated second harmonics is estimated.

## Acknowledgements

This work was supported by Grant-in-Aid for Young Scientists (B) (20760584).

## References

[1] N. Ohyabu, T. Morisaki, S. Masuzaki, R. Sakamoto, M. Kobayashi, J. Miyazawa, M. Shoji, A. Komori, O. Motojimi, and LHD Experimental Group, Phys. Rev. Lett. **97**, 055002 (2006).

[2] Y. Shimomura, R. Aymar, V.A. Chuyanov, M. Huguet, H. Matsumoto, T. Mizoguchi, Y. Murakami, A.R. Polevoi, M. Shimada, Nucl. Fusion **41**, 309 (2001).

[3] Y. Kawano, S. Chiba and A. Inoue, Rev. Sci. Instrum. **72**, 1068 (2001).

[4] T. Akiyama, K. Kawahata, Y. Ito, S. Okajima, K. Nakayama, S. Okamura, K. Matsuoka, M. Isobe, S. Nishimura, C. Suzuki et al., Rev. Sci. Instrum. **77**, 10F118 (2006).

[5] M. A. Van Zeeland, R. L. Boivin, T. N. Carlstrom, and T. M. Deterly, Rev. Sci. Instrum. **79** 10E719 (2008).

[6] Ch. Fuchs and H. J. Hartfuss, Phys. Rev. Lett. **81**, 1626 (1998).

[7] T. Akiyama, K. Kawahata, Y. Ito, S. Okajima, K. Nakayama, S. Okamura, K. Matsuoka, M. Isobe, S. Nishimura, C. Suzuki et al., Rev. Sci. Instrum. **77,** 10F118 (2006).

[8] A. Boboc, L. Zabeo, and A. Murari, Rev. Sci. Instrum. **77**, 10F324 (2006).

[9] V. P. Drachev, Yu. I. Krasnikov and P. A. Bagryansky, Rev. Sci. Instrum. **64** 1010 (1993).

[10] P. A. Bagryansky, A. D. Khilchenko, A. N. Kvashnin *et. al.*, Rev. Sci. Instrum. **77** 053501 (2006).

[11] S. Ya Tochitsky, V. O. Petukhov, V. A. Gorobets, V. V. Chuakov and V. N. Jakimovich, Appl. Optics **36**, 1882 (1997).

[12] Cleverland Crystals Inc.

[13] A. Yariv, "Optical Electronics in Modern Communications fifth edition", Oxford University Press.